Chemical Crystallography and Structural Chemistry

VO 270063-1

Lecture № 8 — 15th June 2023

Dr. Tim Grüne
Centre for X-ray Structure Analysis
Faculty of Chemistry
University of Vienna

tim.gruene@univie.ac.at

Course Schedule

2nd	March	Lecture № 1	9th	March	Lecture № 2
16th	March	Lecture № 3	23th	March	Exercise № 1
30st	March	Lecture № 4	20th	April	Lecture № 5
27th	April	Exercise № 2	4th	May	Lecture № 6
11th	May	Lecture № 7	25th	May	Exercise № 3
1st	June	**no lecture**	15th	June	Lecture № 8
22nd	June	Lecture № 9	29th	June	Exercise № 4

Exercise № 4: Hands-on at the X-ray Centre, Room 2E45/2E46.

Previous Lecture

- Refinement and Model Building
- Restraints and Constraints
- Absolute Configuration

Contents

1 From X-ray Diffraction to Electron Diffraction

Typical (inhouse) X-ray Diffractometer: STOE Stadivari

- X-ray source(s) and detector
- three-axis goniometer for crystal orientation
- Monitor for crystal alignment
- liquid nitrogen stream for cooling to 100 K

Data collection in a nutshell

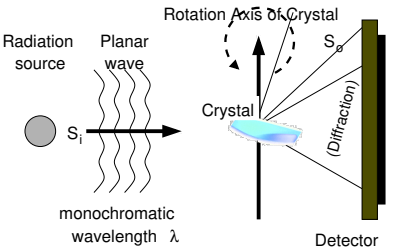

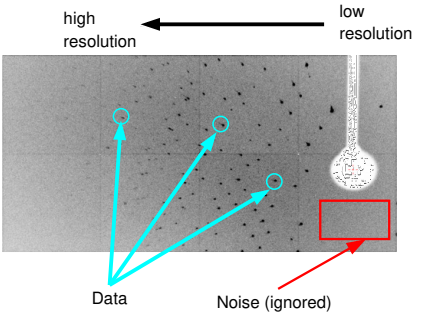

- Monochromatic radiation
- Single crystal
- Crystal rotates during data collection
- Area detector
- Diffraction pattern composed of reflections (“spots”)

Diffraction pattern

- Data collected in “frames”
- Per frame: several reflections
- positions of reflections described by the Laue conditions *via* scattering vector $\vec{S}$, the unit cell vectors, and the Miller indices

$$\vec{S} \cdot \vec{a} = h$$
$$\vec{S} \cdot \vec{b} = k$$
$$\vec{S} \cdot \vec{c} = l$$

- The intensities of the reflections differ with the radiation type. This is relevant for data scaling and model refinement. Data integration is less affected.

From X-ray to electron diffraction

In 3D electron diffraction,
monochromatic, planar X-ray radiation (wavelength $\lambda \approx 1$ Å)
is replaced with
monochromatic, planar electron radiation (wavelength $\lambda \approx 0.025$ Å).
That's all.

Differences between X-ray and Electron Diffraction

Everything so far is the same between X-ray and Electron Diffraction

crystal size (thickness)	5–200 µm	100–1,000 nm
wavelength	1 Å	0.025 Å= 1/40 Å
pressure	ambient	vacuum

2 Theory of Electron Diffraction

Structure factor

The structure factor $F(hkl)$ is *defined* as the Fourier transform of content of the unit cell. "Content" refers to the type of interaction of the radiation:

X-ray $F(hkl) = \int \rho(x,y,z) e^{2\pi i(hx+ky+lz)}$

- $\rho(x,y,z)$: local density of electrons, $[e/\text{Å}^3]$
- High density at atoms, low density away from atoms
- contribution of nuclei irrelevant

ED $F(hkl) = \int \Phi(x,y,z) e^{2\pi i(hx+ky+lz)}$

- $\Phi(x,y,z)$: local electrostratic potential, $[V]$
- Combination of nucleic charge and electron cloud

Structure factor: Crystal and Diffraction experiment

The definition of the structure factor leaves two open questions

1. What is the connection between $F(hkl)$ and the chemical compound inside the crystal?
2. What is the connection between $F(hkl)$ and the diffraction pattern?

Crystal and the Structure Factor — both X-ray and ED

The *Independent Atom Model* (IAM) is a powerful method to calculate the atomic structure factor $F(hkl)$. Each atom contributes independently from the others to $F(hkl)$.

$$F(hkl) = \sum_{\text{in u.c.}}^{\text{atoms } j} f_j(\theta) e^{-8\pi^2 U_j(\theta,\lambda)} e^{2\pi i(hx_j+ky_j+lz_j)} \quad (1)$$

f_j atomic *form* factor. Dependent on atom element, decreases with decreasing scattering angle $\theta = \theta(hkl)$

$U_j(\theta, \lambda)$ atomic displacement parameter (ADP, alias Debye-Waller factor): models thermal vibration of atoms

$e^{2\pi i(hx_j+ky_j+lz_j)}$ phase shift of the atom relative to the origin of the unit cell

Form factor in ED and X-rays

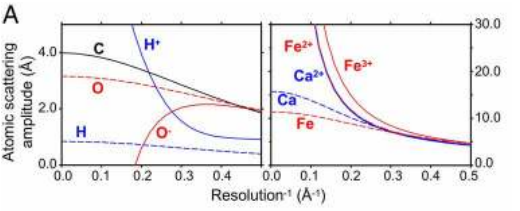

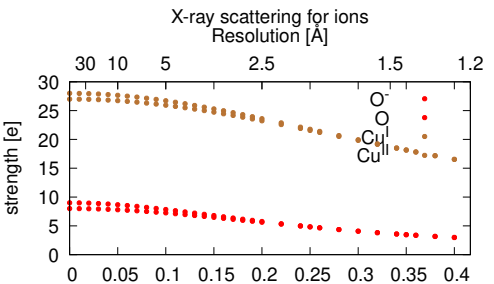

Structure Factor and observed intensities

In the kinematic theory of diffraction for X-rays [1],

$$I_{obs}(hkl) = \frac{e^4}{{m_e}^2 c^4} \frac{\lambda^3 V_{crystal}}{V_{u.c.}^2} I_0 LPTE |F(hkl)|^2$$
$$I_{obs}(hkl) \propto |F(hkl)|^2$$

In electron diffraction, the assumption $I_{obs}(hkl) \propto |F(hkl)|^2$ is less accurate, but still works for many purposes.

Dynamic diffraction [2, 3, 4, 5]

- kinematic diffraction theory: $I_{obs}(hkl) \propto |F(hkl)|^2$ is the "normal" theory
- A better detailed description for $I_{obs}(hkl)$ is based on the *dynamic theory* of diffraction.
- Dynamic calculations are computationally much more demanding than kinematic calculations and for protein structures not very practical.
- Implemented in the refinement program JANA2006
- SHELXL, OLEX2: based on the kinematic diffraction theory
- kinematic theory sufficient for macromolecular structures
- dynamic theory results in better fine details (positions of hydrogen atoms ...)

3 ED Instrumentation

Transmission Electron Microscope as Radiation Source[4, 6, 7]

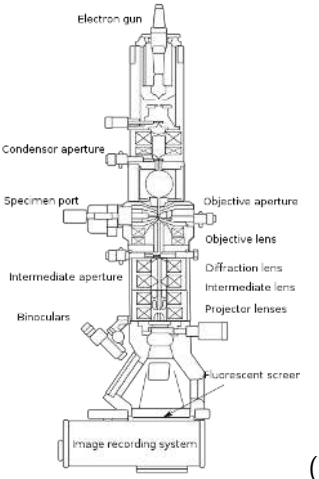

(Wikipedia)

Electron diffractometers

- most groups have been using transmission electron microscopes (TEMs)
- major manufacturers: Hitachi, JEOL, Thermofisher
- JEOL and Thermofisher offer "microED" packages for data collection
- two dedicated electron diffractometers available: Rigaku's SynergyLab-ED and ELDICO's ED-1

ELDICO Scientific: ED-1[8]

- Horizontal beam: goniometer stability $\pm$ 70° (cf. Heidler et al. [9])
- STEM mode for crystal search: no hysteresis from switching between imaging and diffraction; 20 nm resolution
- Dectris hybrid pixel detector, 512x512

RIGAKU XtaLAB Synergy-ED[10]

- based on JEM2100Plus
- RIGAKU CrysAlis^{Pro} software: indicates during data collection, when structure has been solved
- HyPix hybrid pixel detector, 512x512

Our Instrumentation in Vienna

- JEOL JEM2100Plus and Philips CM200 (LaB_6,200 keV)
- PSI JUNGFRAU 1024x512px and DECTRIS QUADRO 512x512 (courtesy University of Basel)
- Current loan: 1024x1024 SINGLA (DECTRIS)

The Lens System [4, 6, 7]

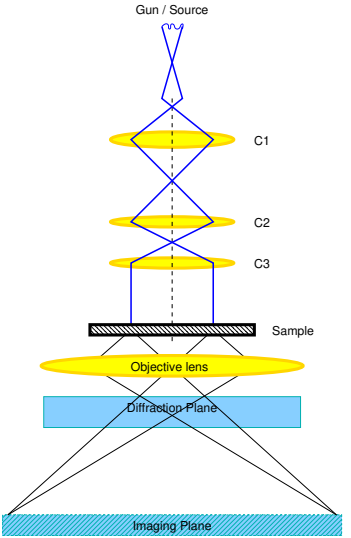

- Lenses C1–C3 shape beam
- Crystallography: Parallel beam
- Objective lens: sets effective detector distance to backfocal plane = diffraction mode
- C3 not present in all microscopes

Imaging and Diffraction in the TEM

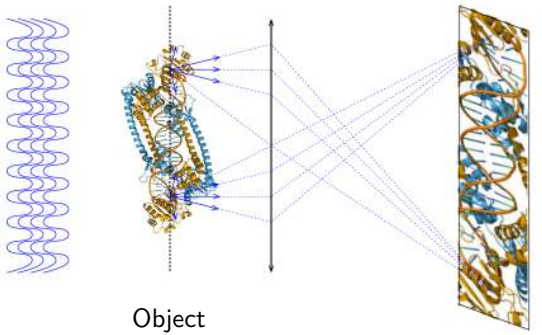

Imaging: Rays of **equal origin** focus on detector

cryo-EM: Imaging Mode

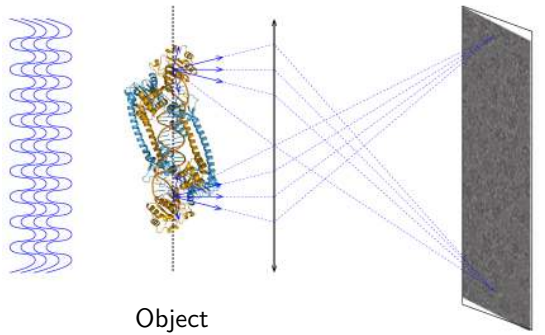

Detector noise and radiation senstivity require low contrast images

Martinez-Rucobo *et al.* Molecular Cell (2015) 58, 1079–1089

Electron Microscope: Diffraction Mode

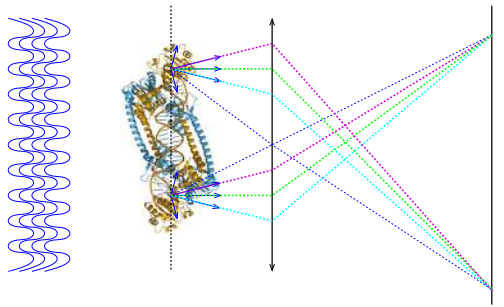

Electron Microscope: Diffraction Mode

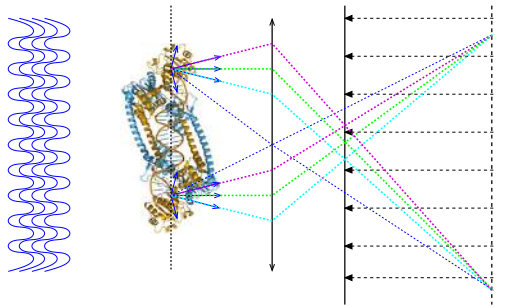

Diffraction: Rays of **equal direction** focus on detector at the backfocal plane

With X-ray diffraction, we can move the detector distance freely to match the resolution limit of the crystal. In a TEM, the detector distance is fixed. We must set the lens system to project the backfocal plane onto the detector plane.

4 ED Sample Preparation

Data collection is your last experiment

(Zbigniew Dauter, National Cancer Institute[11])

Conditions inside the TEM

Two conditions or requirements inside the TEM affect sample preparation for ED:

1. ultra high vacuum, $\leq 10^{-6}$ mbar
2. ultra thin sample thickness, ≤ 1 µm

Ultra high vacuum $\leq 10^{-6}$ mbar

- Sample must be protected from desiccation
- Most common: cool to -180°C
- note: water sublimes at -90°C – -100°C at this pressure
- alternative: suspension in ionic liquid

Ultra thin sample thickness, ≤ 1 µm

- Sample too small for light microscopes
- "blind" sample preparation until inside TEM
- complicates sample preparation

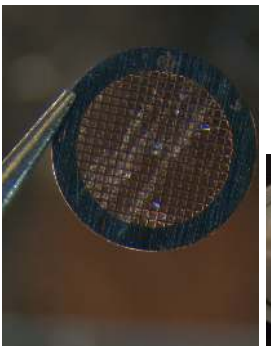

Thin and vacuum: Consequences for sample preparation

Steps from grid until sample can be screened

1. insert grid into holder ($\leq$ 1min)
2. insert holder into TEM ($\leq$ 1min)
3. pre-vaccuum holder chamber (2–5min)
4. start electron beam (2–5min)
5. start screening
6. remove holder (2-3min)

Typically, 5–10 grids are prepared with varying conditions and screened for proper sample size and thickness

TEM grids

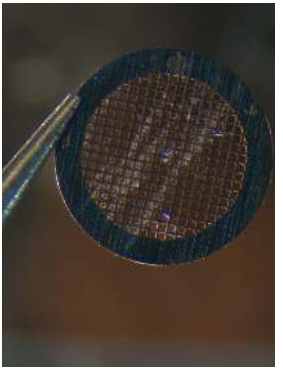

- TEM grid diameter 3 mm
- Metal grid (Cu, Au, Ni) for stability
- sample on mesh between grid-bars

TEM grids film types[1]

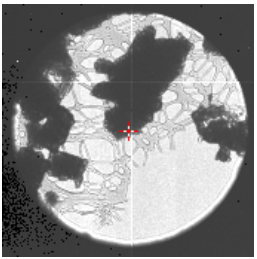

Lacey carbon

Good orientation while scanning the grid

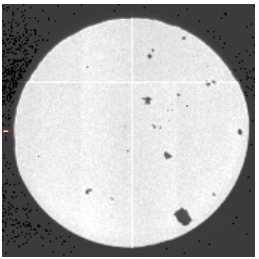

Continuous, amorphous carbon

2-4nm amorphous carbon available: minimum background

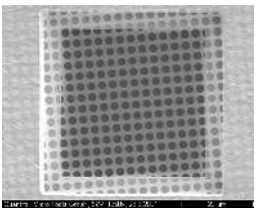

Quantifoil: regular holes with 1-2 µm diameter

Often used in single particle cryoEM

[1] Nicole Bolehradski

Sub-micrometer sized crystals

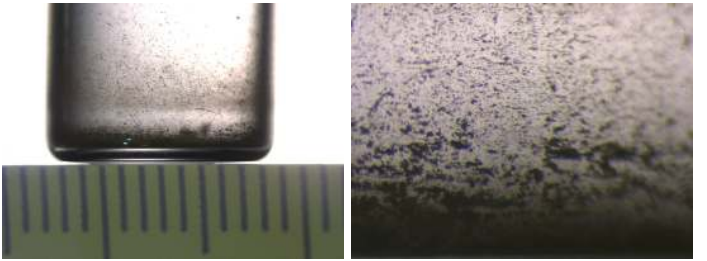

Sample ChWi629 (Christopher Wittmann, University of Vienna, group V. Arion)

- crystals thickness should be $< 1\ \mu m$
- crystals invisible with light microscope
- crystals should be sufficiently isolated to avoid multiple lattices
- crystals should be sufficiently dense to avoid excessive search duration

Sample preparation for powders[12]

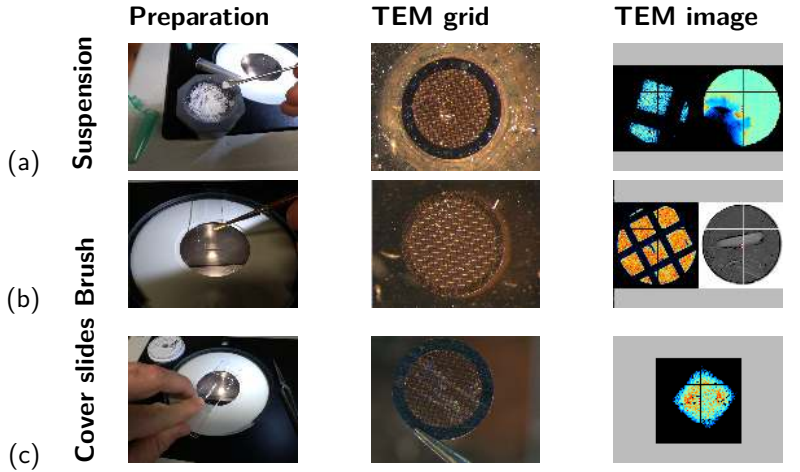

Powders can be dispersed from suspension, with a fine-haired brush, and grounded between cover slides. Often, crystals are still too big for ED.

Tiny mortar: Vortex vial with grid

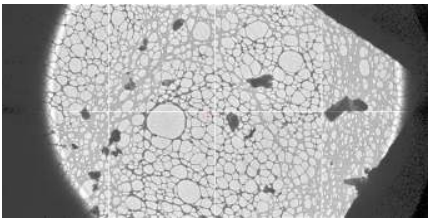

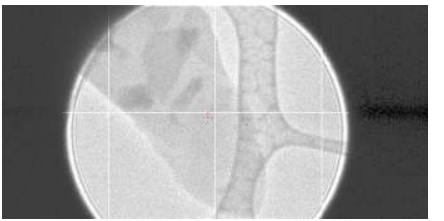

Compatible with dry samples and with suspensions

Classical cryo plunging

1. add drop to grid
2. blot excess liquid with tissue
3. shock-cool in liquid ethane bath

Preassis

"A simple pressure-assisted method for MicroED specimen preparation" [13]

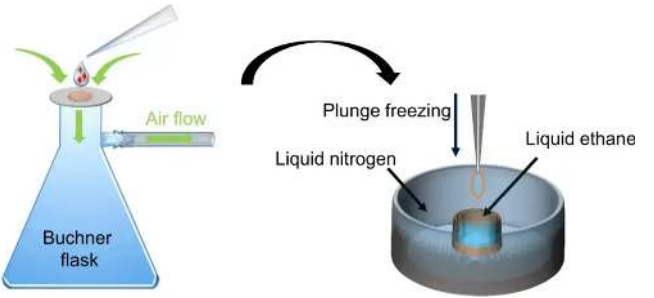

Fig. 1 from Zhao et al. [13]

Desiccation

- Dip sample into suspension **or**
- Drop suspension onto grid
- watch evaporation with light microscope

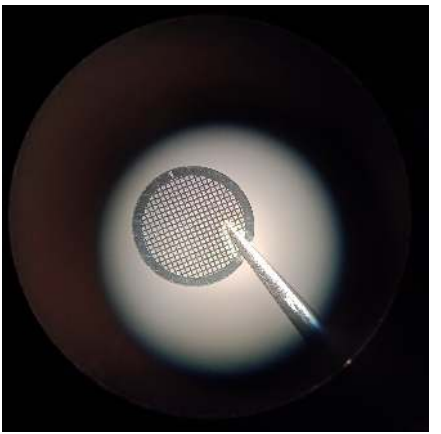

Manual side-blotting

- Dip sample into suspension **or**
- Drop suspension onto grid
- Hold tissue to side of grid
- Watch grid with light microscope

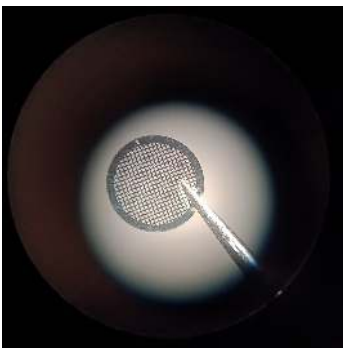

Candidate crystals for ED [14]

- Crystals for ED have to be small — smaller than visible with a light microscope
- Shabby looking crystals might be composed of well-ordered single crystals
- Needles are good candidates for ED

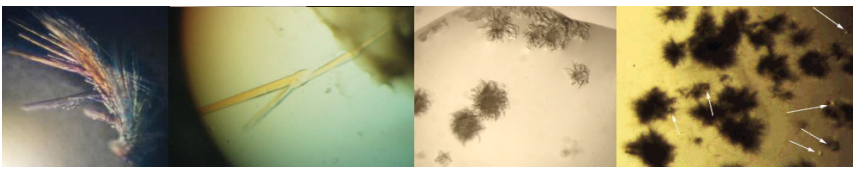

sea urchins (2x right) courtesy Terese Bergfors [14]

5 ED Data Collection

Steps of data collection

1. find crystal
2. centre (align) crystal
3. rotate crystal and collect data

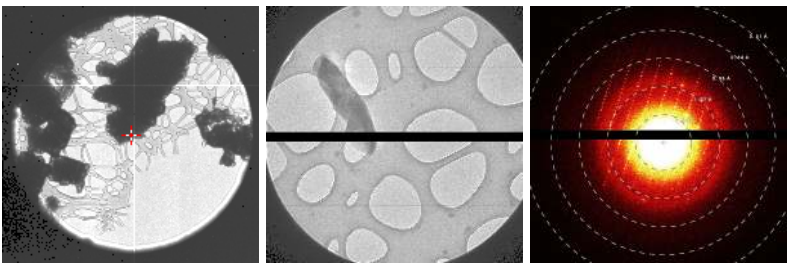

Steps of data collection — finding crystal

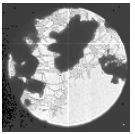

- Isolated, single crystal
- Diffraction quality, beam sensitivity
- Crystal size
  1. adapt beam diameter / magnification to match crystal size
  2. large crystal: easier to centre
- Crystal thickness
  1. too thick: no diffraction
  2. too thin: too much radiation damage

Steps of data collection — centring crystal

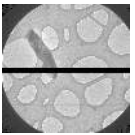

1.3 µm × 390 nm

- Beam diameter ≤ 1µm
- Much higher precision required than for X-ray diffractometers
- Cannot rotate by $90°$: iterative centring required
  - rotate by $\approx 5°$
  - correct crystal drift by shifting height
  - goto step 1

Steps of data collection — collecting data

1. Rotate the holder to the starting position, limited by
   - the instrument, typically $-70°$ or
   - shading by the grid bar (crystal at edge)
   - overlap of other crystals (multiple lattices)

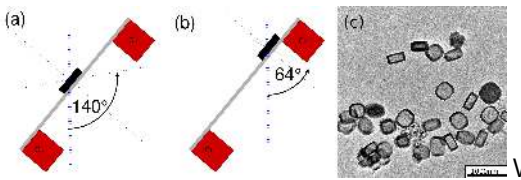

Wennmacher et al. [15, Fig. 1]

Steps of data collection — collecting data

2. Switch to diffraction mode
3. Start rotation
4. Start recording data
5. Process data

6 ED Refinement

Structure Factors

- Experimental **data** after processing: observed intensities $I_{\text{obs}}(hkl)$
- Structural **model** composed of atoms with element type, coordinates (x, y, z), temperature factor B (Debye-Waller factor, ADP)
- Refinement programs (SHELXL, OLEX2) improve the model with respect to the data
- They must compute calculated intensities $I_{\text{calc}}(hkl)$

Computation of intensities $I_{\mathbf{calc}}(hkl)$

- There are several ways to compute $I_{\mathrm{calc}}(hkl)$ from the model
- some are more accurate and more complex
- some are less accurate and fast
- the IAM — independent atom model — assumes scattering from isolated atoms
- atomic scattering factors can be calculated
- the total $I_{\mathrm{calc}}(hkl)$ results from the sum of the individual atoms

Comparison of scattering factors

X

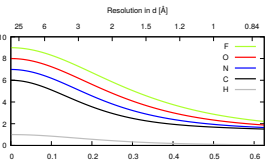

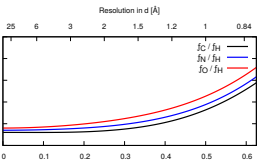

e^-

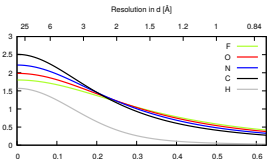

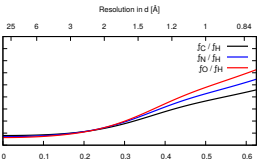

n

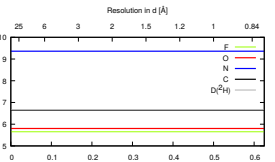

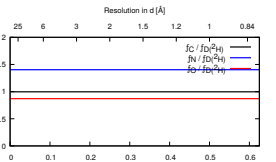

7 ED Examples

Protein crystallisation[16, 17]

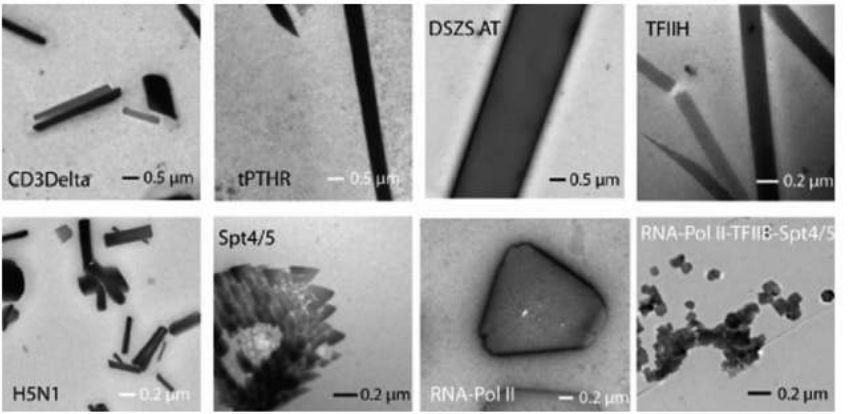

Electron diffraction provides access to many more compounds that seemingly (!) failed crystallisation.

Small Crystals: Jewels in the mud[18]

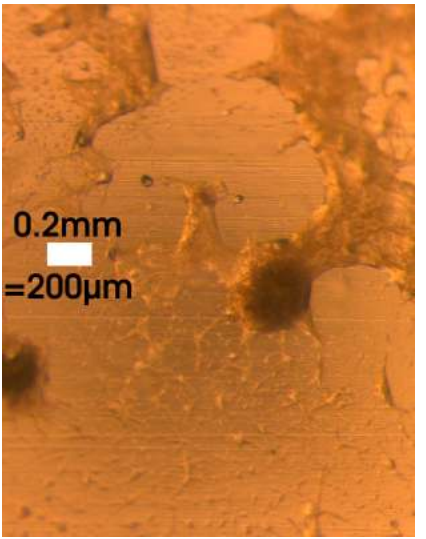

Sample courtesy Jia-Min Chin & Michael Reithofer, photographs courtesy A. Roller

Powerful electron diffraction[18]

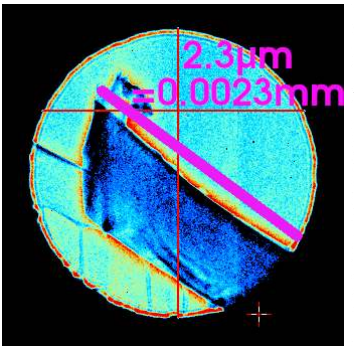

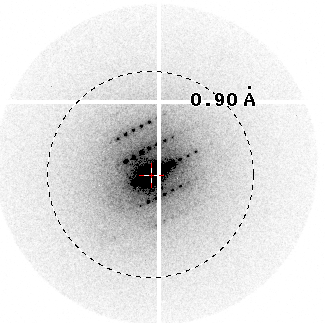

Sample preparation: A. Roller & N. Gajic

At DESY, the strongest X-ray source in the world, this crystal would probably not show any diffraction.

Nd-MOF structure from 5 crystals[18]

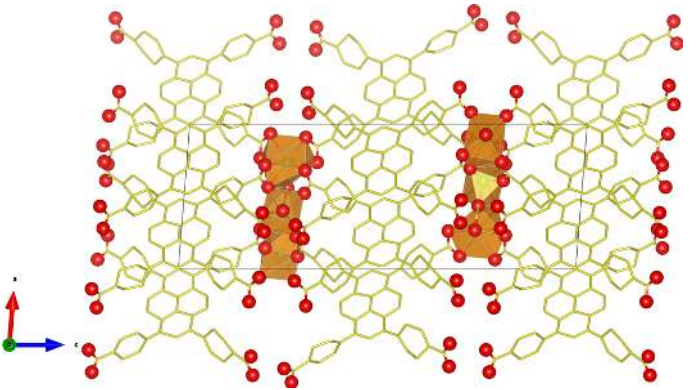

Room temperature measurement, under vacuum

Sub-micrometer sized crystals[19]

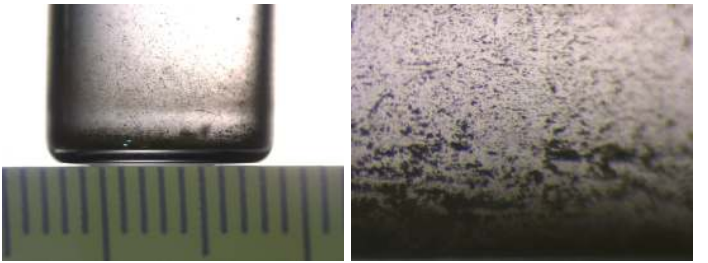

Sample ChWi629 (Christopher Wittmann, University of Vienna, group V. Arion)

Strong diffraction (ChWi629)[19]

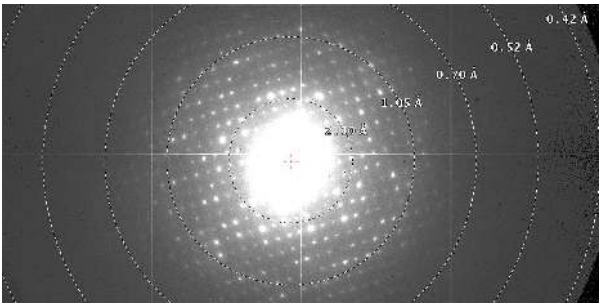

Structure ChWi629[19]

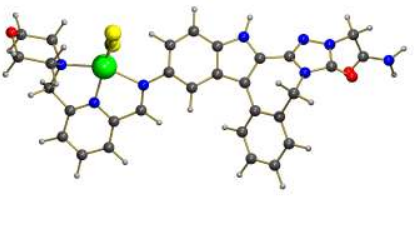

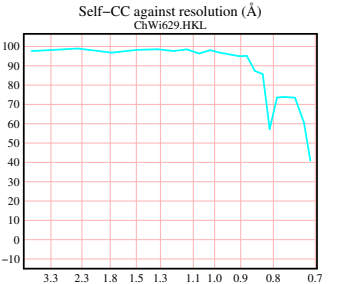

Missing wedge and data quality for ChWi629[19]

RESOLUTION LIMIT	NUMBER OF REFLECTIONS OBS'D	UNIQUE	POSSIBLE	COMPLETENESS OF DATA	I/SIGMA	R-meas	CC(1/2)
3.14	385	101	183	55.2%	7.08	15.4%	97.1*
1.40	4496	1105	1904	58.0%	6.75	16.2%	98.1*
1.11	4963	1205	2095	57.5%	5.69	19.0%	96.8*
0.91	7986	1966	3410	57.7%	4.38	26.5%	96.3*
0.78	7431	2390	4446	53.8%	2.45	45.3%	67.5*
0.70	3910	1614	4663	34.6%	1.70	66.7%	68.2*
total	29171	8381	16701	50.2%	3.85	18.5%	98.2*

Details in Structure ChWi629[19]

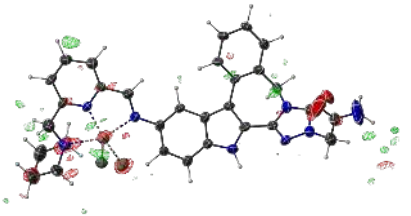

R1 (all) = 23.91 %
R1 (strong) = 18.91 %
wR2 = 48.23 %

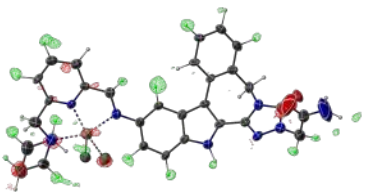

OMIT $H:
R1 (all) = 25.50 %
R1 (strong) = 20.84 %
wR2 = 51.70 %

8 Differentiation between Al and Si with JUNGFRAU

E. Fröjdh et al. 'Discrimination of Aluminum from Silicon by Electron Crystallography with the JUNGFRAU Detector'. In: *Crystals* 10 (2020), p. 1148. DOI: 10.3390/cryst10121148

Hybrid Pixel Detectors[2]

- Hybrid pixel detectors introduced for X-ray crystallography ≈ 2006 (Pilatus[21])
- Soon after recognised as suitable for electron detection[22]
- Medipix consortium (CERN) -> Amsterdam Scientific[23]
- EIGER (both PSI and DECTRIS)[24,25]
- JUNGFRAU as charge integrating detector[20]

[2] slides courtesy Erik Frojdh, PSI detector group

Jungfrau: Photon Counting vs. Charge Integrating[3]

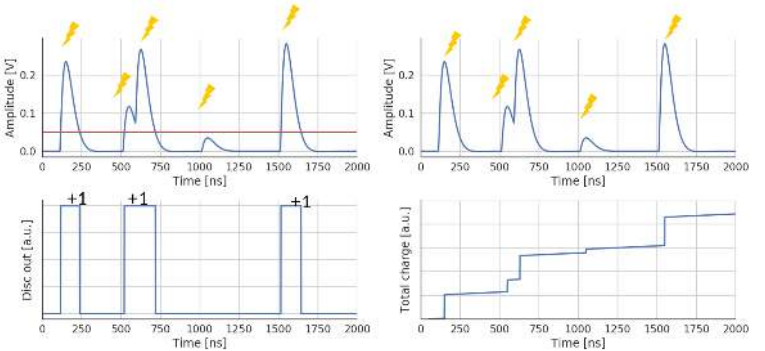

3 photons 37.3 keV

= incoming photon

[3]slides courtesy Erik Frojdh, PSI detector group

X-ray diffraction: Differentiate element types

X-ray structure of sucrose (ordinary sugar)
swapping C for N or O increases R1-value ($\Delta R1/R1 = 0.60$ and 0.18)

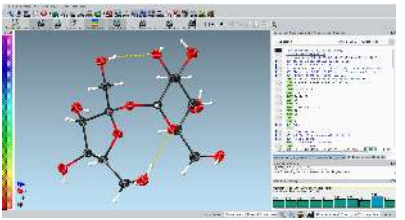

proper: R1=3.21 %

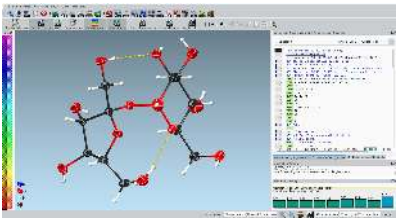

$C1 \rightarrow O$: R1= 5.12 %

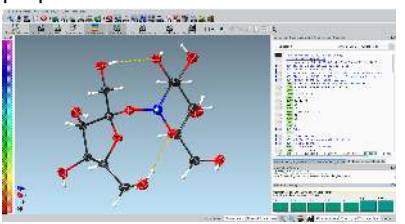

$C1 \rightarrow N$: R1 = 3.79

Benchmarking JUNGFRAU: zeolite A and albite[20]

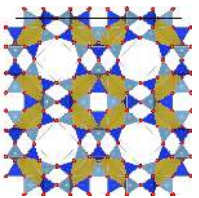

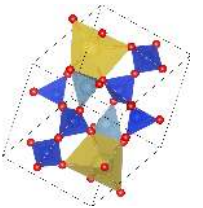

Aluminosilicates, building unit: $Si - O_4$ (T-sites) tetrahedron

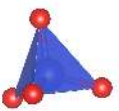

Both zeolite A and albite have one known T-site as Al, rest is Si;

Sodium feldspar mineral albite $NaAlSi_3O_8$

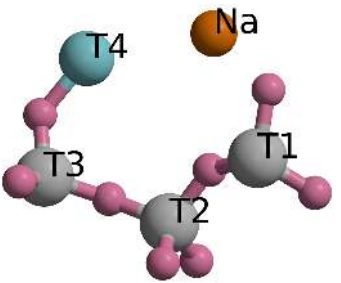

- 4 T sites: 3x Si^{IV}, 1x Al^{III}
- counter ion Na^+
- spacegroup $P1$, 7.13Å, 7.38Å, 7.64Å, ,115.17°, 107.2°, 100.6°
- resolution 6.36Å-0.64Å, 96 % complete
- $R_{\text{complete}} = 23.05\%$
- known Al-position at T4, T1–T3 = Si
- 16 possible assignments of T-sites to Al or Si

Sodium feldspar mineral albite $NaAlSi_3O_8$

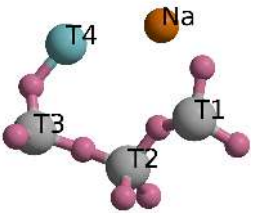

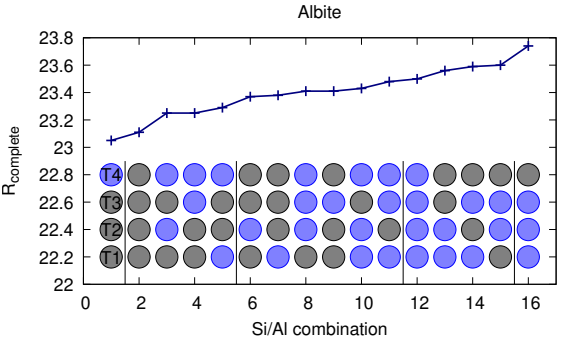

- The correct assignement $T1 = T2 = T3 = Si$ and $T4 = Al$ results in the lowest R_{complete}
- increasing incorrectly assigned sites result in increase of R_{complete}
- Fröjdh et al. [20]

Zeolite A $NaAlSiO_4$

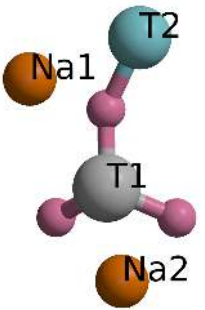

- 2 T sites: 1x Si^{IV}, 1x Al^{III}
- counter ion Na
- spacegroup $Fm\bar{3}c$, $a = 24.5$Å
- resolution 12Å-0.75Å, > 99 % complete per crystal
- 5 individual crystals

Zeolite A $NaAlSiO_4$

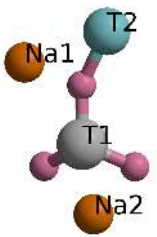

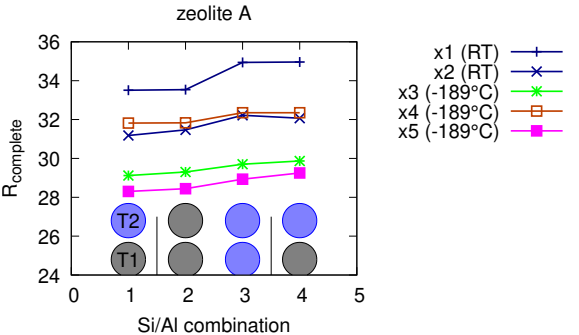

- The correct assignement $T1 = Si$ and $T2 = Al$ results in the lowest R_{complete} in all cases
- increasing incorrectly assigned sites result in increase of R_{complete} in all cases
- Fröjdh et al. [20]

Acknowledgements

- Soheil Mahmoudi, Julian Maisriml, Maria Schmetterer, Nicole Bolehradski, (Chemistry, Uni Vienna)
- R. Miletich-Pawliczek, Chr. Lengauer (Mineralogie, Uni Vienna)
- Julian T. C. Wennmacher, Jeroen A. v. Bokhoven, et al. (ETH Zurich)
- Erik Frojdh, Bernd Schmitt, et al. (PSI Detector Group)
- Julian Holstein (TU Dortmund)
- Swiss Nanoscience Institute
- Sacha DeCarlo, Clemens Schulze-Briese (Dectris Ltd.)

Julian Wennmacher, Soheil Mahmoudi

References

[1] C. Giacovazzo, ed. *Fundamentals of Crystallography*. Oxford University Press, 1985.

[2] J. Jansen et al. '*MSLS*, a Least-Squares Procedure for Accurate Crystal Structure Refinement from Dynamical Electron Diffraction Patterns'. In: *Acta Crystallogr.* A54 (1998), pp. 91–101.

[3] A. Authier. *Dynamical Theory of X-Ray Diffraction*. IUCr Monographs on Crystallography. Oxford University Press Inc., New York, 2001.

[4] L. Reimer and H. Kohl. *Transmission Electron Microscopy*. Physics of Image Formation. Springer-Verlag New York, 2008. ISBN: 978-0-387-34758-5.

[5] Lukáš Palatinus, Václav Petříček and Cinthia Antunes Corrêa. 'Structure refinement using precession electron diffraction tomography and dynamical diffraction: theory and implementation'. In: *Acta Crystallogr* A71 (2015), pp. 235–244.

[6] C. B. Carter and D. B. Williams. *Transmission Electron Microscopy. Diffraction, Imaging, and Spectrometry*. Springer International Publishing Switzerland, 2016. ISBN: 978-3-319-26651-0.

[7] J. M. Zuo and J. C. H. Spence. *Advanced Transmission Electron Microscopy. Imaging and Diffraction in Nanoscience*. Springer Science+Business Media New York 2017, 2016. ISBN: 978-1-4939-6607-3.

[8] ELDICO Scientific. *ED-1*. URL: https://www.eldico-scientific.com (visited on 08/05/2022).

[9] Jonas Heidler et al. 'Design guidelines for an electron diffractometer for structural chemistry and structural biology'. In: *Acta Crystallogr* D75 (2019), pp. 458–466. DOI: 10.1107/S2059798319003942.

[10] RIGAKU. *XtaLAB Synergy-ED*. URL: https://www.rigaku.com/products/crystallography/synergy-ed (visited on 08/05/2022).

[11] Zbigniew Dauter. 'Data-collection strategies'. In: *Acta Crystallogr.* D55 (1999), pp. 1703–1717. DOI: 10.1107/S0907444999008367.

[12] Tim Gruene et al. 'Establishing electron diffraction in chemical crystallography'. In: *Nat. Rev. Chem.* (2021), pp. 660–668. DOI: 10.1038/s41570-021-00302-4.

[13] Jingjing Zhao et al. 'A simple pressure-assisted method for MicroED specimen preparation'. In: *Nat. Commun.* 12 (2021), p. 5036. DOI: 10.1038/s41467-021-25335-7.

[14] T. Bergfors. *Terese Bergfors — Protein Crystallization*. URL: https://xray.teresebergfors.com/ (visited on 26/02/2021).

[15] Julian T. C. Wennmacher et al. '3D-structured supports create complete data sets for electron crystallography'. In: *Nat. Commun.* 10 (2019), p. 3316.

[16] Hilary P. Stevenson et al. 'Use of transmission electron microscopy to identify nanocrystals of challenging protein targets'. In: *Proc. Natl. Acad. Sci. U. S. A.* 111 (2014), p. 8470. DOI: 10.1073/pnas.1400240111.

[17] Guillermo Calero et al. 'Identifying, studying and making good use of macromolecular crystals'. In: *Acta Crystallogr* F70 (2014), pp. 993–1008. DOI: 10.1107/S2053230X14016574.

[18] Tim Gruene et al. 'CELLOPT: improved unit-cell parameters for electron diffraction data of small-molecule crystals'. In: *J. Appl. Crystallogr.* 55 (2022), pp. 647–655. DOI: 10.1107/S160057672200276X.

[19] Christopher Wittmann et al. 'Latonduine-1-Amino-Hydantoin Hybrid, Triazole-Fused Latonduine Schiff Bases and Their Metal Complexes: Synthesis, X-ray and Electron Diffraction, Molecular Docking Studies and Antiproliferative Activity'. In: *Inorganics* 11 (2023). URL: https://doi.org/10.3390/inorganics11010030.

[20] E. Fröjdh et al. 'Discrimination of Aluminum from Silicon by Electron Crystallography with the JUNGFRAU Detector'. In: *Crystals* 10 (2020), p. 1148. DOI: 10.3390/cryst10121148.

[21] Ch. Broennimann et al. 'The PILATUS 1M detector'. In: *J. Synchrotron Radiat.* 13 (2006), pp. 120–130.

[22] G. McMullan et al. 'Detective quantum efficiency of electron area detectors in electron microscopy'. In: *Ultramicroscopy* 109 (2009), pp. 1126–1143. DOI: https://doi.org/10.1016/j.ultramic.2009.04.002.

[23] M. T. B. Clabbers et al. 'Protein structure determination by electron diffraction using a single three-dimensional nanocrystal'. In: *Acta Crystallogr.* D73 (2017), pp. 738–748. DOI: 10.1107/S2059798317010348.

[24] G. Tinti et al. 'Electron Crystallography with the EIGER detector'. In: *IUCrJ* 5 (2018), pp. 190–199. DOI: 10.1107/S2052252518000945.

[25] Tim Gruene et al. 'Rapid structure determination of microcrystalline molecular compounds using electron diffraction'. In: *Angew. Chem., Int. Ed.* 57 (2018), pp. 16313–16317. DOI: 10.1002/anie.201811318.